3 August 2001

ELSEVIER

Chemical Physics Letters 343 (2001) 241–250

CHEMICAL PHYSICS LETTERS

www.elsevier.com/locate/cplett

Graphitic cones in palladium catalysed carbon nanofibres

H. Terrones [a,b,c], T. Hayashi [c], M. Muñoz-Navia [a,d], M. Terrones [a,e,*], Y.A. Kim [c], N. Grobert [e], R. Kamalakaran [f], J. Dorantes-Dávila [d], R. Escudero [g], M.S. Dresselhaus [h], M. Endo [c]

[a] *IPICyT, Venustiano Carranza 2425-A, Col. Los Filtros, 78210 San Luis Potosí, SLP, México*
[b] *Instituto de Física, Laboratorio Juriquilla, UNAM A.P. 1-1010, 76000 Querétaro, México*
[c] *Shinshu University, Faculty of Engineering, Wakasato, Nagano-city, 380-8553, Japan*
[d] *Instituto de Física 'Manuel Sandoval Vallarta', UASLP, 78000 San Luis Potosí, SLP, México*
[e] *Fullerene Science Centre, School of Chemistry, Physics and Environmental Science, University of Sussex, Falmer, Brighton BN1 9QJ, UK*
[f] *Max-Planck-Institut für Metallforschung, Seestr. 92, D-70174 Stuttgart, Germany*
[g] *Instituto de Investigaciones en Materiales, UNAM, A.P.70-360, 01000 México, D.F, México*
[h] *Massachusetts Institute of Technology, Cambridge, MA 02139-4307, USA*

Received 16 May 2001; in final form 8 June 2001

Abstract

High yields of graphitic conical nanofibres (5–70 nm OD; <5 μm long) are produced by pyrolysing palladium precursors under Ar at 850–1000°C. The fibres exhibit diamond-shaped Pd particles at their tips, which are responsible for the formation of stacked graphene cones (open, lampshade-type, or closed). The cones observed with apex angles of ca. 30°, 50° and 70° can be explained by an open cone approach, which considers different chiralities. Due to the presence of open edges (dangling bonds), we envisage that these novel nanofibres may find important applications in the fabrication of field emitters, gas storage components and composites.

1. Introduction

The identification of carbon nanotubes (CNTs) [1] has propelled a new area of carbon nanomaterials, which is expected to have important implications for the development of electronic devices, flat panel displays, robust composites, nano-switches, etc. [2–6]. These results prove that carbon is very flexible and is able to form not only CNTs (multi- or single-walled), but also fullerenes [7], graphitic onions [8], toroids [9], boxes [10], and cones [11–13]. In this Letter we report a simple route to synthesize a new type of graphitic conical nanofibre by pyrolysing solid Pd compounds. Our results also demonstrate that Pd can be used as an efficient catalyst for the formation of carbon nanostructures.

Early theoretical studies predicted the formation of graphitic cones [14,15]. Subsequently, isolated graphitic cones were produced by carbon condensation on a graphite substrate [11] and by pyrolysis of heavy oils [12]. More recently, single-walled aggregates of conical graphitic structures have been prepared by laser ablation of graphite targets [13]. In addition, conical structures

* Corresponding author. Fax: +44-1273-677196.
E-mail address: mterrones@titan.ipicyt.edu.mx (M. Terrones).

0009-2614/01/$ - see front matter
PII: S0009-2614(01)00718-7

consisting of other layered materials such as BN have also been prepared by reacting boron oxide vapours with multi-walled CNTs (MWCNTs) [16].

It has been shown that carbon fibres can be efficiently produced by pyrolysing hydrocarbons over metal catalysts such as Fe, Co and Ni [17,18]. These catalysts usually form carbides and have been intensively used in the production of carbon nanofibres, nanotubes [19–21] and Fe nanowires [22,23]. It is noteworthy that pyrolytic methods are advantageous when compared to arc-discharge [24] and electrolysis techniques [25] because the growth conditions and quality of the resulting material can be controlled [26]. However, Pd has not been used as a catalyst for the formation of carbon nanofibres, possibly because it is reluctant to form stable carbide phases. In this account, we also demonstrate that Pd plays a crucial role in the formation of a high yield of graphitic conical nanofibres using a simple pyrolytic process. Catalytic disproportionation of CO, using Ni supported on alumina–silica mixtures with different H_2 amounts, can produce open edge graphitic structures similar to stacked cone arrays [27]. Recently, La_4PdO_7 was used as a precursor in order to produce Pd nanoparticles, and under certain conditions, the authors noticed that carbon nanofibres were also obtained. These experiments were carried out under a controlled flux of CO and He at 650°C, followed by long heat treatments and tedious separation processes (e.g., isolation of La_2O_3 from the carbon nanostructures) [28]. It is noteworthy that our conical fibres are produced in the absence of toxic gases such as CO and other impurities such as La.

The graphitic cones in our fibres exhibit apex angles from 32° to 82°, which can be explained in terms of open conical graphene sheets (lampshade-type), have also been observed by Kiselev et al. [29]. According to theoretical calculations, closed graphene cones exhibit a charge transfer to the pentagonal rings (at the caps) [30], which could be important in the development of field emission sources. However, open cones may exhibit enhanced field emission properties (caused by the open edge sites) as well as Aharonov–Bohm magnetic effects and magnetoconductance [31]. We believe that localised states at the Fermi level (for the open cones) may give rise to materials with novel electronic and magnetic properties [32].

2. Experimental

The pyrolysis of Pd precursors was carried out in the presence of Ar using a two-stage furnace system coupled with temperature controllers [22]. Powders (10–50 mg) of palladium acetyl–acetonate ($[CH_3COCH{=}C(O)CH_3]_2Pd$, Aldrich, 99%), palladium acetate ($[CH_3CO_2]_2Pd$, Aldrich, 98%) or dichloro (1,5-cyclooctadiene) palladium ($C_8H_{12}Cl_2$ Pd, Aldrich, 99%), were inserted in one end of a quartz tube (80 cm long; 6 mm i.d.). Subsequently, the tube was placed in a two-stage furnace and the region containing the powder sample was located outside the furnaces. Ar flows (5–15 cm^3/min) were then passed through the tube and the two furnaces were heated (50°C/min) to the set temperature (from 450°C to 1050°C in 100°C steps). At this temperature, the tube was moved so that the region containing the powder was introduced into the first furnace region. This promoted a fast (<10 s) reaction, which caused the deposition of carbonaceous materials in the region of the first and the second furnaces. The furnaces were left operating for an additional 15 min in order to anneal the products.

Deposits scratched from the tube walls (both furnaces) were then analysed using scanning electron microscopy (SEM; JEOL JSM-6335F operating at 3–15 kV and a Zeiss DSM 982 Gemini operated at 1–2 kV). Minute amounts of the powder samples (1–2 mg) were then dispersed ultrasonically (5–30 min) in 5 ml acetone, and a few drops of the dispersions were placed on a holey carbon grid for transmission electron microscopy studies. High-resolution transmission electron microscopy (HRTEM) measurements were carried out in a JEOL JEM-2010FEF operated at 200 kV (equipped with an omega filter, a Gatan multiscan camera and an energy dispersive X-ray – EDX – Oxford Ins. detector), a JEOL JEM-4000 microscope operating at 400 kV and a JEOL JEM-3000F microscope operated at 300 kV (equipped with an EDX Noran Ins. detector).

Raman spectra were recorded at room temperature under ambient conditions using a Renishaw Raman Image Microscope System 1000 equipped with a CCD multi-channel detector. The excitation source consisted of an Ar-ion laser (514.5 nm). The laser beam (0.8 μm spot size) was focused on the sample using an optical microscope (objective lens of 100×). During spectra acquisition, the optical power was maintained at 5 mW in order to avoid any signal shifts of the spectra and sample damage caused by local overheating. The scattered light was collected in a backscattering configuration. The peak frequencies of the Raman spectra were determined by fitting the raw data with a Lorentzian distribution function. The Raman spectral lines were obtained with an accuracy $>\pm 2$ cm^{-1}.

3. Results and discussion

SEM and TEM studies reveal that the material collected from the furnace consists of entangled nanofibres exhibiting 'diamond-shape' metal particles at their tips (Fig. 1). These fibres seem to grow radially from a common central site (Fig. 1b). From TEM observations, we find Pd multiple-twinned clusters (some of them exhibit with decahedral shapes), surrounded by disordered graphite layers (Figs. 1, 3 and 4). We commonly observe regions in which these Pd twin nanocrystals fragment into 'diamond-shape' particles. Electron diffraction (ED) patterns from these decahedral twinned particles exhibit fivefold symmetry containing the (1 1 1) ($d_{111} = 2.24$ Å) and (0 0 2) ($d_{002} = 1.94$ Å) Pd planes, with the [1 1 0] direction being the zone axis (Figs. 1e,f and 4c,d).

For the three pyrolysed precursors, we noted that large yields of nanofibres were favoured above 850°C, however, fibres start forming at 650°C. The fibres exhibit diameters ranging from 5 to 70 nm and lengths up to 5 μm. TEM observations revealed that all fibres exhibit stacked cone morphologies (Figs. 1, 3 and 4) and a Pd particle (detected by EDX and ED), firmly attached at the tip, even after a 30 min sonication treatment. It is noteworthy that all Pd particles in the fibres exhibit triangular and diamond-like shapes.

The cone angles within different fibres have been measured by ED, taking the fast Fourier transform (FFT) of several micrographs. We observed that angles between 32° and 82° were mainly present. It is important to mention that angles around 40°, 60° and 80° might correspond to 240°, 180° and 120° disclinations in graphite [16], respectively. From a theoretical standpoint, closed graphene cones can be generated by introducing $n = 1$ to 5 pentagonal carbon rings within the hexagonal framework. Using this definition, cone angles can take values given by: $\theta = 2 \times \arcsin(1 - n/6) = 112.8°,\ 83.62°,\ 60°,\ 38.94°$ and 19.188°. However, angles at ca. 30°, 50° and 70°, forbidden by the closed cone approach [12,16], can only be explained in terms of an open cone model. Thus, with an open apex, the cone becomes less rigid and more possibilities for conical graphitic geometries can be envisaged such as the great variety of chiral configurations (Fig. 2).

Once the open cones are formed, their closure can be achieved by introducing defects such as pentagons. In our fibres, if the cones are closed, it is likely that the final closure occurs at the apex. Therefore, the open cone approach supports the formation of our structures and explains the variety of angles observed (Fig. 3).

High-energy electron irradiation studies at high temperatures (not shown here) have demonstrated that open cones can be closed, thus avoiding dangling bonds and preserving the original cone topology (conical angle). It is commonly observed that at the opposite end of the conical fibres (opposite to the Pd triangular-shaped particle at the tip), Pd clusters of round (not triangular) morphologies appear. This observation suggests that the carbon fragmentation/precipitation, and fibre growth only occurs on the triangular (conical) Pd particles. Moreover, broken nanofibres exhibiting closed conical arrangements at the fibre ends (opposite to the Pd triangular particle; Fig. 4) are also observed. From high-resolution TEM images, we notice that the graphite cones always adopt the shape of the conical catalyst particles.

According to our observations, the following growth scenario (see Fig. 5) can be proposed: (i) At 850°C, Pd and carbon clusters form; (ii) Pd clusters aggregate in order to create multiple-twinned

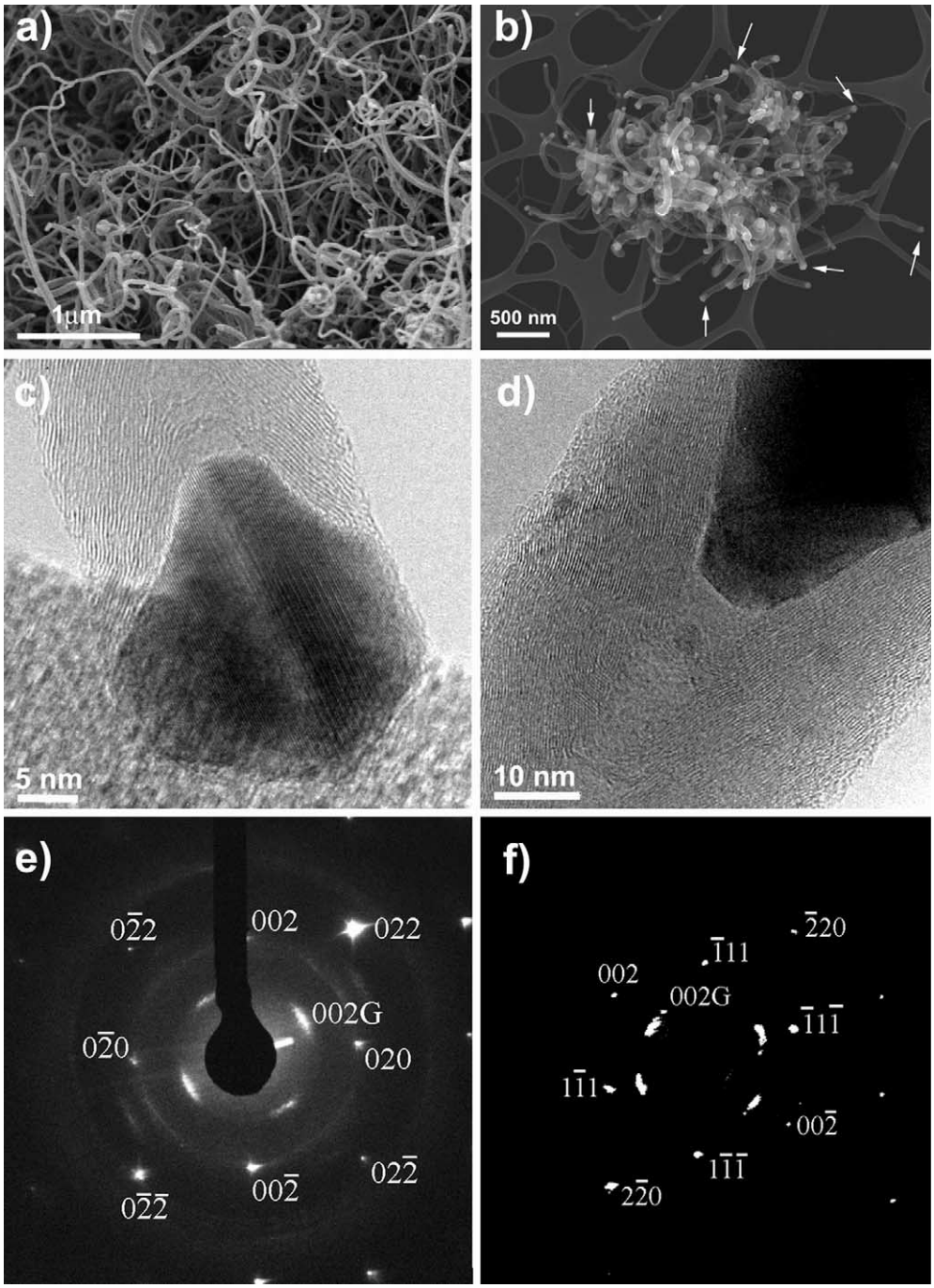

Fig. 1. (a) SEM images of entangled Pd grown carbon nanofibres; (b) SEM image of entangled nanofibres (deposited on a TEM grid) in which the arrows show conical Pd particles at the tips; (c) and (d) HRTEM images of typical Pd particles located at the tip of the fibres (note the conical arrangement of graphene layers); (e) and (f) ED patterns of the conical fibres close to the Pd tip particle. Note that the (0 0 2) reflections of graphite form an 'X' shape, related to the cone apex angle. No preferred orientation between the graphene and the Pd planes was observed. In (e) the Pd zone axis is [1 0 0], whereas in (f) the zone axis is [1 1 0].

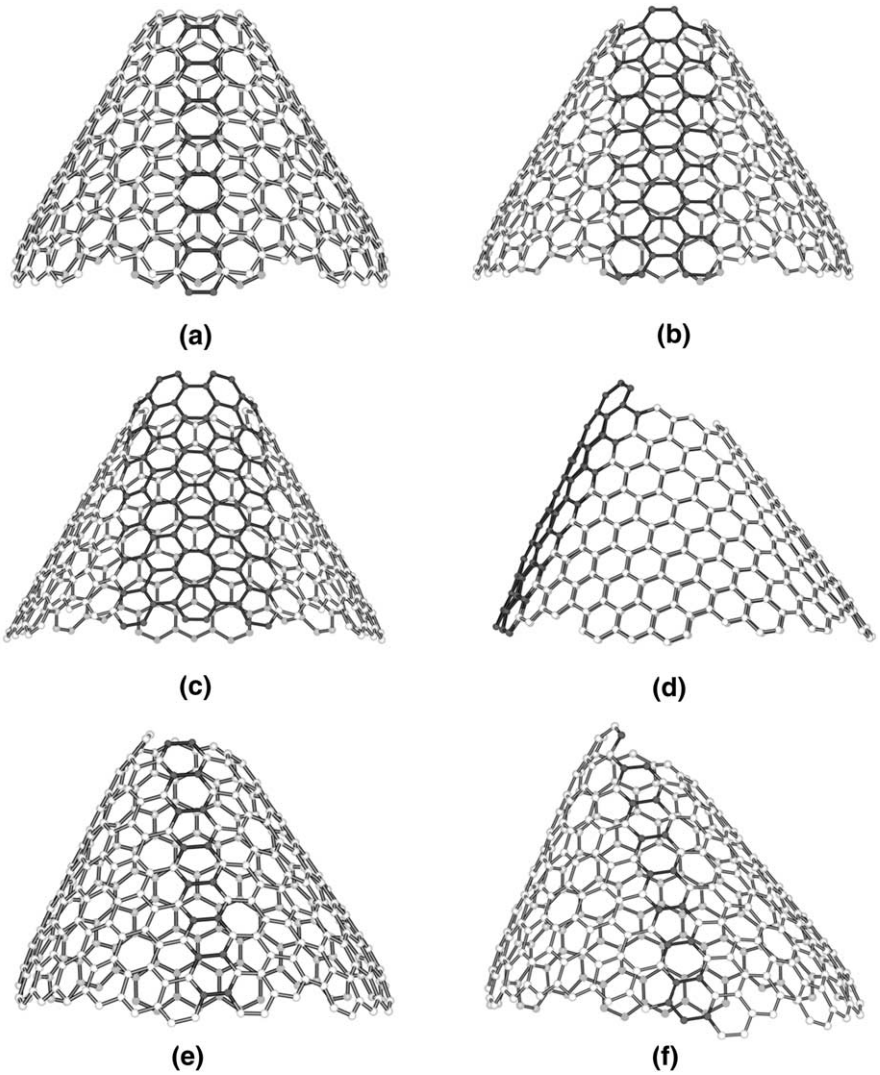

Fig. 2. Various types of open 'graphitic' cones with apex angles ca. 60° (lampshade structures): (a) open cone obtained by removing a 180° sector from a planar graphite sheet; (b) since the cone shown in (a) is open, one layer of hexagons (dark atoms) can be introduced in order to modify the structure and symmetry; (c) three layers of hexagons have been added to the cone depicted in (a) (dark atoms); (d) side view of (c) revealing the asymmetry of the cone with respect to the cone axis (frequently observed in the samples); (e) and (f) by opening the cones [along the dark atoms in (a)], it is possible to form a chiral cone by sliding the edges, thus forming new structures (note the different angle of the dark atoms).

particles (see also Fig. 4d), which can be either decahedral or icosahedral; (iii) carbon species interact with the hot Pd polygonal cluster and diffuse along the exposed surface and between the grain boundaries, thus fragmenting the twin crystals into tetrahedral-like and diamond-shaped Pd particles; (iv) carbon diffuses, on the exposed conical Pd particles, and precipitates at the other end, thus forming graphite cones; (v) carbon continues to diffuse, creating 'fresh' cones, which displace the previously formed cones by releasing stress between the cones and the Pd particle; (vi) the carbon aggregation continues and the conical fibre is created (Fig. 5).

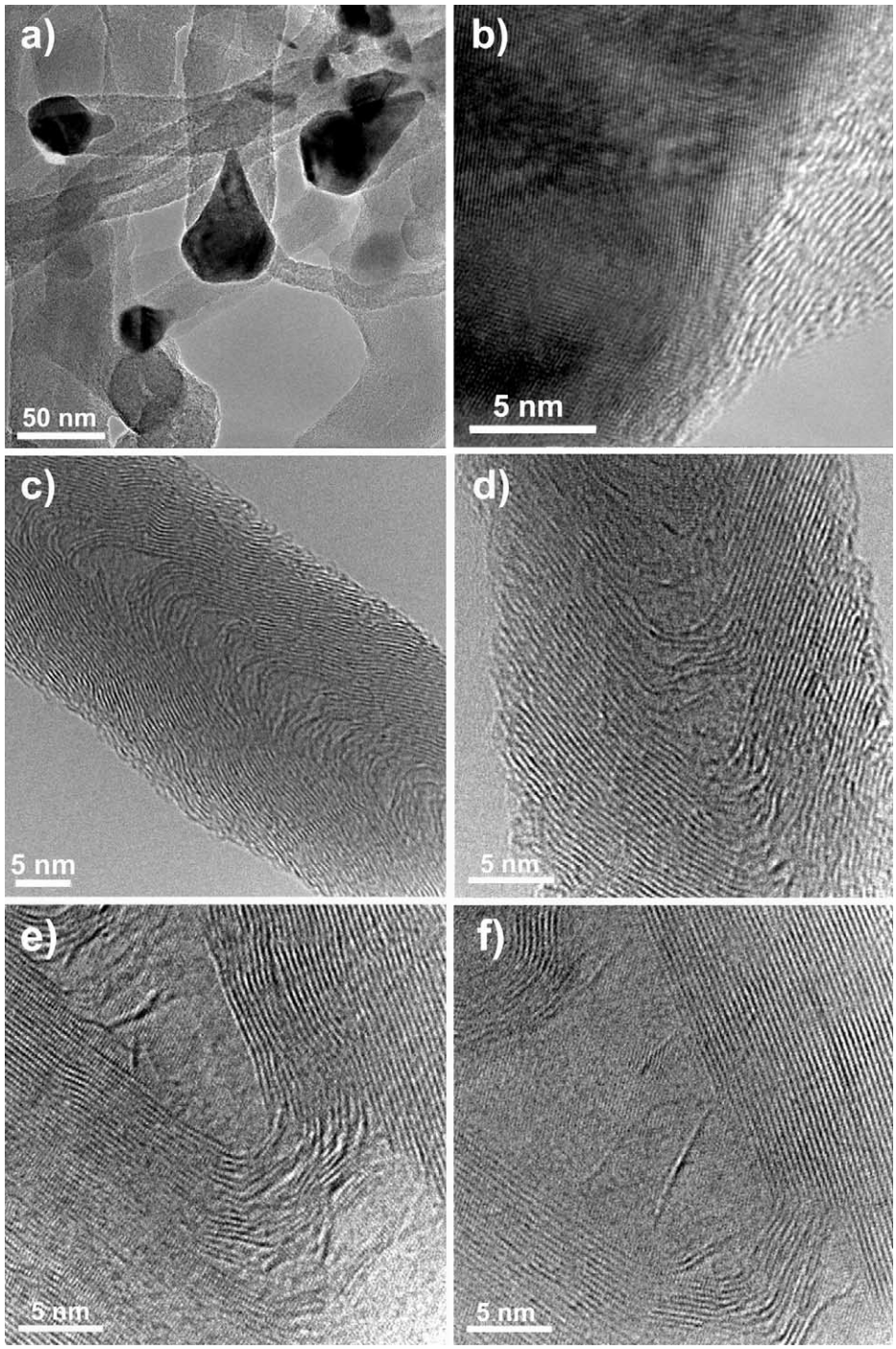

Fig. 3. (a) TEM image of various conical nanofibres exhibiting 'diamond-shape' Pd particles at the tips; (b) HRTEM image of an individual fibre tip showing the Pd [1 0 0] and the graphite [0 0 2] planes, note that these planes do not show a clear epitaxial correlation; (c)–(f) HRTEM images of Pd grown nanofibres exhibiting different conical morphologies. Note that the degree of graphitisation differs from fibre to fibre. The tips of the individual cones are frequently ill-formed, and occasionally the cones are open.

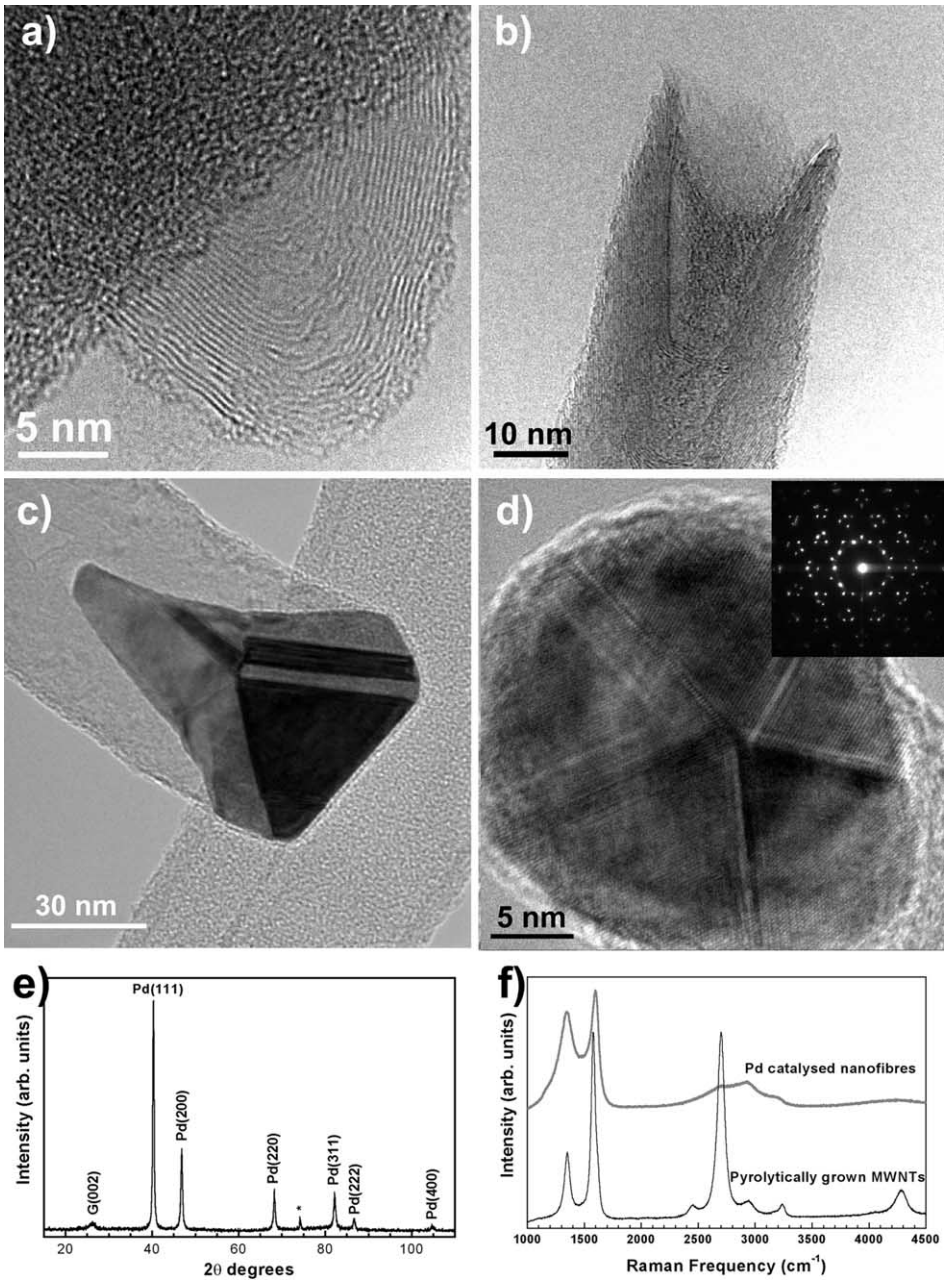

Fig. 4. (a) HRTEM image of a nanofibre showing a closed conical tip, which is located on the opposite side of the Pd catalyst; (b) a nanofibre tip that lost the Pd catalyst particle, possibly by sonication treatment (see the conical interior); (c) TEM image of a conical nanofibre exhibiting a Pd 'conical' particle, which shows twinning in the interior (possibly caused by the fragmentation of larger Pd particles exhibiting decahedral symmetry (shown in d); (d) Pd decahedral cluster with five fold symmetry (inset shows the ED pattern of this particle); (e) X-ray powder diffraction pattern of the whole sample. The graphite 0 0 2 distance corresponds to 3.42 Å and the Pd corresponds to FCC Pd with a lattice parameter of 3.89 Å (* corresponds to minute concentrations of SiO_x phases, possibly arising from the pyrolytic substrate); (f) Raman spectrum of the whole sample showing typical graphitic features and the presence of disorder. For comparison, a highly ordered sample of MWCNTs obtained by pyrolysis of ferrocene is shown.

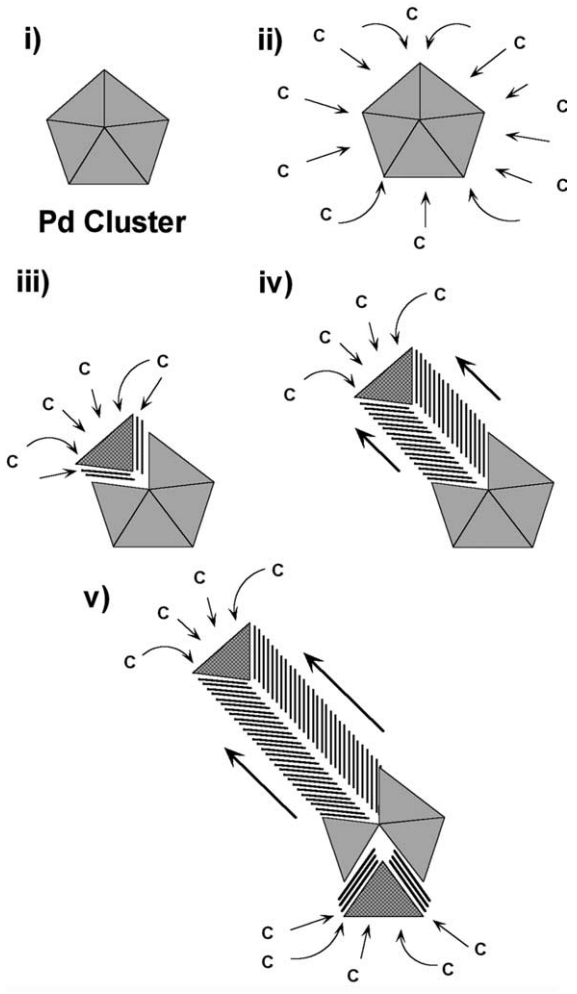

Fig. 5. Possible growth mechanism for the conical nanofibres: (i) Pd clusters form and aggregate in order to create multiple-twinned particles (decahedral or icosahedral, see also Fig. 4d); (ii) carbon species interact with the hot Pd polygonal cluster and diffuse along the exposed surface and between the grain boundaries, thus fragmenting the twin crystals into tetrahedral-like and diamond-shaped Pd particles; (iii) carbon diffuses, on the exposed conical Pd particles, and precipitates at the other end, thus forming graphite cones; (iv–v) carbon continues to diffuse, creating 'fresh' cones, which displace the previously formed cones by releasing stress between the cones and the Pd particle, thus creating the conical fibres.

A decahedral $Pd(D_{5h})$ twin can be formed by introducing 10 distorted Pd tetrahedral crystals, and an icosahedral (I_h) twin should possess 20 of these tetrahedra [33]. In this context, the Pd catalyst initial shape might be related to these tetrahedral crystals whose faces and sharp edges are suitable for carbon diffusion, thus forming the graphene layers that mimic the shape of the catalyst particle creating cones (note that Pd is reluctant to form stable carbides and the diffusion is likely to occur just on the surface). Subsequent carbon deposition will cause the formation of additional cones, which will push the particle up, building in this way the fibre (Fig. 3). We believe that a reshaping of the catalytic particle during the growth process occurs because the exposed surface always exhibits round morphologies, whereas the interior is faceted, perhaps due to the temperature gradient.

As explained previously, these cones can be either open or closed depending on the healing ability of graphite to eliminate dangling bonds at the ends. Therefore, the cone angle and the morphology of the fibre is imposed by the catalytic particle and not by the apex of the cone, which has been proposed for other closed conical graphites and nitrogenated carbon nanofibres [11–13,34].

ED direct measurements using HRTEM micrographs and FFT patterns from different regions of the fibres, indicate that the distance between graphene layers varies from 3.38 to 3.54 Å (average value of 3.45 Å, which is close to that of turbostratic graphite). On some occasions, the (1 0 0) planes of graphite can be distinguished ($d_{(1\,0\,0)} = 0.21$ nm). This observation may be caused by the superposition of graphene cones with an alternating AB... stacking. We envisage that high-temperature thermal treatments would possibly reorient the cones in order to exhibit interlayer distances close to that of graphite (3.35 Å). Therefore, having a stacking similar to graphite (AB...) can make these fibres more suitable for the intercalation of different host species.

We have identified the composition of the metal particles using ED, EDX and X-ray powder diffraction techniques. The results clearly indicate the presence of Pd (Fig. 4e) since the observed structure is similar to that of bulk Pd (FCC; lattice parameter of 3.89 Å). ED studies from these Pd particles exhibit different crystallographic orientations: the [1 1 0], [1 0 0] and [1 1 1] zone axes were identified as well as other arbitrary orientations. ED patterns show that graphitic (0 0 2) planes can

be parallel to the (1 1 1), (0 2 0) and (0 0 2) Pd planes. This observation indicates that a preferred orientation of the Pd planes with respect to the graphite (0 0 2) does not take place. Nevertheless, a detailed analysis is being carried out in order to study the relationship between the orientation of the Pd and graphene planes (Fig. 3b).

Electron energy loss spectra (EELS) on the conical nanofibres reveal typical features of sp^2 carbon, thus confirming their 'graphitic' nature. The Raman spectrum exhibits the characteristic features of graphitic structures, with a G-peak centered at 1598.2 cm^{-1} (1582.1 cm^{-1} for ordered MWCNTs obtained by pyrolysis of ferrocene [22,35], see Fig. 4f) and the D-peak at 1348.2 cm^{-1} (1352.5 cm^{-1} for ordered MWCNTs obtained by pyrolysis of ferrocene [22,35]). The intensity ratio R (I_D/I_G) in our samples is ca. 0.847 (0.338 for highly-ordered MWCNTs obtained by pyrolysis of ferrocene [22,35], though this value can be lowered by the spray pyrolysis method to ~0.232 [35]). These results indicate that the concentric graphene cones of the fibres possess more disorder (e.g., lack of straightness in the graphene layer) when compared to other MWCNTs obtained by pyrolysis. Heat treatment at high temperatures (2500°C), will definitely enhance the straightness of the graphene conical layers and will decrease the I_D/I_G ratio.

4. Conclusion

Conical graphitic nanofibres have been synthesised by pyrolysing three different carbon-contained palladium precursors in the temperature range 850–1000°C. All fibres exhibit stacked cone shape with conical palladium particles, firmly attached, at their tips. The absence of nested cylindrical CNTs is also noteworthy. In these fibres, the shape of the graphene layers is imposed by the shape of the catalytic particle. The conical angles observed in our study can be explained by invoking an open cone approach, which provides more possibilities for illustrating the structure of graphitic cones. The cones within the fibres are held together by van der Waals forces acting between the graphene layers.

We envisage that these fibres may behave as stable field emitters operating at low voltages. Moreover, by using heavy grinding of this material, it may be possible to fragment the fibres into smaller cones. The structures also exhibit compartments between cones which may be advantageous for gas storage. Palladium metal has proved to be useful for H_2 storage; therefore, the metal at the tips may well enhance the H_2 absorption. Theoretical predictions on these novel lampshade fibres may reveal intriguing electronic and magnetic effects. Moreover, this technique can be also used to generate Pd clusters with a determined shape and morphology, which may be advantageous in catalysis.

Acknowledgements

The authors are grateful to M. Rühle, Ph. Redlich, T. Seeger and H. Labitzke for stimulating discussions and technical assistance. We are also indebted to JEOL-Japan for technical assistance and support (M. Kawasaki, M. Shibata, T. Oikawa and T. Osada). H.T. acknowledges the support of the Japanese Society for the Promotion of Science (JSPS Grant No. S-00247) and the hospitality of Shinsu University, Japan, where he has been a visiting scientist. M.T. and H.T. are grateful to CONACYT-México grants: 25237, J31192U and W-8001-millenium initiative, and DGAPA-UNAM grant 108199. M.M.N. and J.D.D. acknowledge IMP-Mexico grant FIES-98-101-I, CONACYT grant 32085-E, M.M.N. thanks CONACyT-México for the Ph.D. grant and N.G. is grateful to The Royal Society for financial support.

References

[1] S. Iijima, Nature (London) 354 (1991) 56.
[2] M. Bockrath, D.H. Cobden, P.L. McEuen, N.G. Chopra, A. Zettl, R.E. Smalley, Science 275 (1997) 1922.
[3] S.J. Tans, A.R.M. Verschueren, C. Dekker, Nature (London) 393 (1998) 49.
[4] Y-K. Kwon, D. Tománek, S. Iijima, Phys. Rev. Lett. 82 (1999) 1470.
[5] T.W. Ebbesen, Phys. Today 49 (6) (1996) 26.
[6] B.I. Yakobson, R.E. Smalley, Am. Sci. 83 (1997) 324.

[7] H.W. Kroto, J.R. Heath, S.C. O'Brien, R.F. Curl, R.E. Smalley, Nature 318 (1985) 162.
[8] D. Ugarte, Nature (London) 359 (1992) 707.
[9] J. Liu J, H.J. Dai, J.H. Hafner, D.T. Colbert, R.E. Smalley, S.J. Tans, C. Dekker, Nature (London) 385 (1997) 780.
[10] Y. Saito, T. Matsumoto, Nature (London) 392 (1998) 237.
[11] M. Ge, K. Sattler, Chem. Phys. Lett. 220 (1994) 192.
[12] A. Krishnan, E. Dujardin, M.M.J. Treacy, J. Hugdahl, S. Lynum, T.W. Ebbesen, Nature (London) 388 (1997) 451.
[13] S. Iijima, M. Yudasaka, R. Yamada, S. Bandow, K. Suenaga, F. Kokai, K. Takahashi, Chem. Phys. Lett. 309 (1999) 165.
[14] H. Terrones, J. Math. Chem. 15 (1994) 143.
[15] A.T. Balaban, D.J. Klein, X. Liu, Carbon 32 (1994) 357.
[16] L. Bourgeois, Y. Bando, W.Q. Han, T. Sato, Phys. Rev. B 61 (2000) 7686.
[17] M.S. Dresselhaus, G. Dresselhaus, K. Sugihara, I.L. Spain, H.A. Goldberg, Graphite Fibers and Filaments, Springer, Heidelberg, 1988.
[18] M. Endo, K. Takeuchi, K. Kobori, K. Takahashi, H.W. Kroto, A. Sarkar, Carbon 33 (1995) 873.
[19] M. Audier, M. Coulon, Carbon 23 (1985) 317.
[20] A. Thess, R. Lee, P. Nikolaev, H. Dai, P. Petit, J. Robert, C. Xu, Y.H. Lee, S.G. Kim, A.G. Rinzler, D.T. Colbert, G.E. Scuseria, D. Tománek, J.E. Fischer, R.E. Smalley, Science 277 (1997) 1971.
[21] C. Journet, W.K. Maser, P. Bernier, A. Loiseau, M.L. Delachapelle, S. Lefrant, P. Deniard, R. Lee, J.E. Fischer, Nature (London) 388 (1997) 756.
[22] N. Grobert, W.K. Hsu, Y.Q. Zhu, J.P. Hare, H.W. Kroto, D.R.M. Walton, M. Terrones, H. Terrones, Ph. Redlich, M. Rühle, R. Escudero, F. Morales, Appl. Phys. Lett. 75 (1999) 3363.
[23] N. Grobert, M. Mayne, M. Terrones, J. Sloan, R.E. Dunin-Borkowski, R. Kamalakaran, T. Seeger, H. Terrones, M. Rühle, D.R.M. Walton, H.W. Kroto, J.L. Hutchison, Chem. Commun. 5 (2001) 471.
[24] T.W. Ebbesen, P.M. Ajayan, Nature (London) 358 (1992) 220.
[25] W.K. Hsu, L.P. Hare, M. Terrones, H.W. Kroto, D.R.M. Walton, P.J.F. Harris, Nature (London) 377 (1995) 687.
[26] M. Terrones, N. Grobert, J. Olivares, J.P. Zhang, H. Terrones, K. Kordatos, W.K. Hsu, J.P. Hare, P.D. Townsend, K. Prassides, A.K. Cheetham, H.W. Kroto, D.R.M. Walton, Nature (London) 388 (1997) 52.
[27] J. Jiao, P.E. Nolan, S. Seraphin, A.H. Cutler, D.C. Lynch, J. Electrochem. Soc. 143 (1996) 932.
[28] M. Adersson, P. Alberius-Henning, K. Jansson, M. Nygren, J. Mater. Res. 15 (2000) 1822.
[29] N.A. Kiselev, J. Sloan, D.N. Zakharov, E.F. Kukovitskii, J.L. Hutchison, J. Hammer, A.S. Kotosonov, Carbon 36 (1998) 1149.
[30] S. Berber, Y.-K. Kwon, D. Tománek, Phys. Rev. B 62 (2000) R2291.
[31] P.E. Lammert, V.H. Crespi, Phys. Rev. Lett. 85 (2000) 5190.
[32] K. Nakada, M. Fujita, G. Dresselhaus, M. Dresselhaus, Phys. Rev. B 54 (1996) 17954.
[33] A.L. Mackay, Acta Cryst. 15 (1962) 916.
[34] V.D. Blank, I.G. Gorlova, J.L. Hutchison, N.A. Kiselev, A.B. Ormont, E.V. Polyakov, J. Sloan, D.N. Zakharov, S.G. Zybtsev, Carbon 38 (2000) 1217.
[35] R. Kamalakaran, M. Terrones, T. Seeger, Ph. Kohler-Redlich, M. Rühle, Y.A. Kim, T. Hayashi, M. Endo, Appl. Phys. Lett. 77 (2000) 3385.